Erroneous ribosomal RNAs promote the generation of antisense ribosomal siRNA

Chengming Zhu[a,1], Qi Yan[a,1], Chenchun Weng[a], Xinhao Hou[a], Hui Mao[a], Dun Liu[a], Xuezhu Feng[a,2], and Shouhong Guang[a,b,2]

[a]Hefei National Laboratory for Physical Sciences at the Microscale, School of Life Sciences, University of Science and Technology of China, Hefei, 230027 Anhui, People's Republic of China; and [b]Chinese Academy of Sciences (CAS) Center for Excellence in Molecular Cell Science, Chinese Academy of Sciences, Hefei, 230027 Anhui, People's Republic of China

Edited by Gary Ruvkun, Massachusetts General Hospital, Boston, MA, and approved August 20, 2018 (received for review January 21, 2018)

Ribosome biogenesis is a multistep process, during which mistakes can occur at any step of pre-rRNA processing, modification, and ribosome assembly. Misprocessed rRNAs are usually detected and degraded by surveillance machineries. Recently, we identified a class of antisense ribosomal siRNAs (risiRNAs) that down-regulate pre-rRNAs through the nuclear RNAi pathway. To further understand the biological roles of risiRNAs, we conducted both forward and reverse genetic screens to search for more suppressor of siRNA (*susi*) mutants. We isolated a number of genes that are broadly conserved from yeast to humans and are involved in pre-rRNA modification and processing. Among them, SUSI-2(ceRRP8) is homologous to human RRP8 and engages in m1A methylation of the 26S rRNA. C27F2.4(ceBUD23) is an m7G-methyltransferase of the 18S rRNA. E02H1.1(ceDIMT1L) is a predicted m6(2)Am6(2)A-methyltransferase of the 18S rRNA. Mutation of these genes led to a deficiency in modification of rRNAs and elicited accumulation of risiRNAs, which further triggered the cytoplasmic-to-nuclear and cytoplasmic-to-nucleolar translocations of the Argonaute protein NRDE-3. The rRNA processing deficiency also resulted in accumulation of risiRNAs. We also isolated SUSI-3(RIOK-1), which is similar to human RIOK1, that cleaves the 20S rRNA to 18S. We further utilized RNAi and CRISPR-Cas9 technologies to perform candidate-based reverse genetic screens and identified additional pre-rRNA processing factors that suppressed risiRNA production. Therefore, we concluded that erroneous rRNAs can trigger risiRNA generation and subsequently, turn on the nuclear RNAi-mediated gene silencing pathway to inhibit pre-rRNA expression, which may provide a quality control mechanism to maintain homeostasis of rRNAs.

rRNA | risiRNA | *N*1-methyladenosine | 7-methylguanosine | Nrde

One of the functional cores of ribosomes is rRNA, which promotes the assembly of ribosomes and catalyzes mRNA decoding and amino acid polymerization (reviewed in refs. 1–5). In eukaryotic cells, rRNAs are transcribed by RNA polymerase I into a single 47S polycistronic precursor in the nucleolus. Pre-rRNAs are then modified, processed, folded, and matured into 18S, 5.8S, and 28S rRNA; 5S rRNA is independently transcribed by RNA polymerase III in the nucleus. During the biogenesis process, rRNAs are extensively modified in the nucleolus, nucleus, and cytoplasm by small nucleolar RNA (snoRNA)-dependent or -independent enzymes (6, 7). These modifications stabilize the structure of the ribosomes and facilitate efficient and accurate protein synthesis.

Due to the crucial roles of ribosomes, cells must carefully surveil every step of ribosome formation from pre-rRNA processing to the assembly of ribosomal subunits to avoid accumulating harmful RNAs (8). Misprocessed rRNAs are usually detected and degraded by multiple surveillance machineries, including the exosome and Trf4/Air2/Mtr4p polyadenylation (TRAMP) complexes (1, 4, 9–11). The exosome plays a key role in 3′-5′ exonucleolytic decay of aberrant RNAs (12–14). The exosome-independent exoribonuclease SUSI-1 (ceDIS3L2) is involved in 3′–5′ degradation of oligouridylated RNA fragments (15, 16).

In addition to enzymatic degradation to remove erroneous rRNAs, antisense ribosomal siRNAs (risiRNAs) can down-regulate pre-rRNA through the nuclear RNAi pathway in *Caenorhabditis elegans* (16). risiRNAs belong to the 22G-RNA category and exhibit sequence complementarity to 18S and 26S rRNAs. risiRNAs bind to both cytoplasmic and nuclear Argonaute proteins to silence rRNA expression. When the exoribonuclease SUSI-1 (ceDis3L2) is mutated, risiRNAs are dramatically increased (16). However, the biological significance of risiRNAs is still unclear. It is unknown whether environmental stimuli can activate certain signaling pathways to elicit risiRNA production and how the defects in rRNA degradation machinery can lead to risiRNA generation.

To further understand the biological roles and generation mechanism of risiRNAs, in this study, we isolated a series of mutants in which risiRNAs were accumulated by forward and reverse genetic screens and CRISPR-Cas9–mediated gene knockout technology. Many of the isolated genes are highly conserved from yeast to humans and are involved in rRNA modification and pre-rRNA processing. Thus, we concluded that misprocessed rRNAs or modification deficiency in rRNAs may promote the generation of risiRNAs, which can act in a feedback loop to maintain cellular rRNA homeostasis via the nuclear RNAi pathway.

Results

Genetic Screen Identified Antisense risiRNAs That Accumulated in the *susi-2* Mutant. NRDE-3 is an Argonaute protein that transports siRNAs from the cytoplasm to the nucleus. NRDE-3 localizes to the nucleus when it binds to siRNAs but accumulates in the cytoplasm in the absence of siRNA ligands (17). Impairments in the generation of endogenous siRNAs, for example, in the *eri-1*

Significance

Ribosome biogenesis is a very sophisticated multistep process, in which mistakes can occur at any step during pre-rRNA processing, modification, and the assembly of ribosomal subunits. Here, we identified a pathway in which erroneous rRNAs promote the generation of ribosomal siRNAs, which further recruit the nuclear RNAi machinery to suppress the accumulation of erroneous rRNA. Our observations pinpointed a layer of gene regulation in which rRNA processing and the RNAi pathway are connected with each other to maintain rRNA homeostasis.

Author contributions: C.Z., Q.Y., X.F., and S.G. designed research; C.Z., Q.Y., C.W., X.H., H.M., and D.L. performed research; C.Z. and Q.Y. contributed new reagents/analytic tools; C.Z., Q.Y., and C.W. analyzed data; and X.F. and S.G. wrote the paper.

The authors declare no conflict of interest.

This article is a PNAS Direct Submission.

Data deposition: The dataset of small RNA deep sequencing reported in this paper has been deposited in the Gene Expression Omnibus (GEO) database, https://www.ncbi.nlm.nih.gov/geo (accession no. GSE113905).

[1]C.Z. and Q.Y. contributed equally to this work.

[2]To whom correspondence may be addressed. Email: fengxz@ustc.edu.cn or sguang@ustc.edu.cn.

This article contains supporting information online at www.pnas.org/lookup/suppl/doi:10.1073/pnas.1800974115/-/DCSupplemental.

mutant result in relocalization of NRDE-3 from the nucleus to the cytoplasm. Using the subcellular localization of GFP::NRDE-3 as a reporter, we designed genetic screen strategies to search for factors that negatively regulate endo-siRNA generation in *C. elegans*. We chemically mutagenized *eri-1(mg366);GFP::NRDE-3* worms and isolated mutants that were capable of redistributing NRDE-3 from the cytoplasm to the nucleus by a clonal screen. Previously, we reported that SUSI-1 (ceDis3L2) acts as a key exonuclease involved in the 3′–5′ degradation of oligouridylated rRNAs (16, 18). To further understand the biogenesis of risiRNAs, we investigated *susi-2* and *susi-3*, two evolutionarily conserved genes that are involved in pre-rRNA methylation and processing.

One allele of *susi-2(ust49)* was isolated from this screen. In the control *eri-1(mg366);GFP::NRDE-3* animals, NRDE-3 localized in the cytoplasm. In *eri-1(mg366);susi-2(ust49);GFP::NRDE-3* animals, NRDE-3 accumulated in the nucleus (Fig. 1*A*). We mapped *susi-2(ust49)* to *t07a9.8* by SNP mapping and genome resequencing, in which the -1 guanosine was mutated to adenine right before the ATG codon, while the predicted ORF remained intact (*SI Appendix*, Fig. S1*A*). To confirm that *susi-2* is *t07a9.8*, we used CRISPR-Cas9 technology to create an allele, *susi-2(ust50)*, which also resulted in the nuclear localization of GFP::NRDE-3 (Fig. 1*A* and *SI Appendix*, Fig. S1*A*). Additionally, we used the dCAS9 system (19) to knockdown *t07a9.8* and observed the cytoplasmic-to-nuclear translocation of NRDE-3 in *eri-1 (mg366);GFP::NRDE-3;susi-2(dCAS9)* animals (Fig. 1*A*). We then generated a single-copy mCherry-fused SUSI-2 transgene driven by the *nrde-3* promoter via the mosSCI technology, introduced it back into *eri-1(mg366);susi-2(ust49);GFP::NRDE-3*, and rescued the cytoplasmic localization of NRDE-3 (*SI Appendix*, Fig. S1*B*). Therefore, we conclude that *susi-2* is the *t07a9.8* gene. Because the homozygous allele of *susi-2(ust50)* is lethal, we used *susi-2(ust49)* as the reference allele in the following studies.

To test whether NRDE-3 associated with risiRNAs in the *susi-2* mutant, we immunoprecipitated NRDE-3 and deep sequenced NRDE-3–bound small RNAs in a 5′-phosphate–independent manner. risiRNAs distributed among 18S to 26S ribosomal DNA regions and increased ∼140-fold in *eri-1(mg366);susi-2(ust49);GFP::NRDE-3* animals compared with wild-type animals (Fig. 1 *B* and *C* and *SI Appendix*, Fig. S1*C*). Notably, the proportion of NRDE-3–bound risiRNAs rose from 0.3% in control animals to 43% in the *susi-2* mutants (*SI Appendix*, Fig. S1*D*). The majority of risiRNAs started with a guanosine at the 5′ end and were 22 nt in length, suggesting that they were 22G-RNAs (*SI Appendix*, Fig. S1*E*) (20). To further show that risiRNAs were specifically increased in the *susi-2* mutants, we deep sequenced total small RNAs from both control and *eri-1(mg366);susi-2(ust49);*GFP::NRDE-3 animals. The number of risiRNA reads was approximately fivefold higher in *eri-1(mg366);susi-2(ust49);*GFP::NRDE-3 than in control animals (*SI Appendix*, Fig. S1*F*).

To search for the genetic requirements of risiRNA production in the *susi-2* mutant, we crossed a number of available mutants onto the *eri-1(mg366);susi-2(ust49);*GFP::NRDE-3 animals. *rrf-2*, *drh-3*, and *rde-12*, which are important for the generation of secondary endo-siRNAs, were required for risiRNA production (16). In these mutants, NRDE-3 partially relocalized to the cytoplasm. While NRDE-3 mainly accumulated in the nucleus in the *rrf-1* mutant, NRDE-3 markedly redistributed into the cytoplasm in the *rrf-1;rrf-2* double mutant (*SI Appendix*, Fig. S1*G*). We used qRT-PCR to quantify risiRNAs and confirmed that the generation of risiRNAs is strongly suppressed in *rrf-1;rrf-2* double mutants (Fig. 1*D*). These results suggested that risiRNAs belong to the secondary siRNA category and require RNA-dependent RNA polymerases (RdRPs) for production.

FIB-1 encodes the *C. elegans* ortholog of human fibrillarin and *Saccharomyces cerevisiae* Nop1p (21). FIB-1 localizes to the nucleolus in embryos. In the *susi-2* mutant, NRDE-3 colocalized with mCherry::FIB-1, suggesting that NRDE-3 translocated to the nucleoli and that risiRNAs may thereby silence rRNAs in the nucleoli (Fig. 1*E*). Additionally, NRDE-3 associated with pre-rRNA in *susi-2(ust49)* mutants (*SI Appendix*, Fig. S1*H*).

Low temperature has been shown to up-regulate risiRNA production (16). We quantified the nuclear localization of NRDE-3 in different culture conditions and found that NRDE-3 accumulated in the nucleus at 15 °C and 20 °C but not at 25 °C in *eri-1(mg366);susi-2(ust49)* animals. Using qRT-PCR, we confirmed that low temperature (15 °C and 20 °C) but not high temperature (25 °C) promoted risiRNA production in *susi-2(ust49)* animals (*SI Appendix*, Fig. S1 *I* and *J*).

SUSI-2 Is Required for the m1A Modification of rRNAs. *susi-2* is located in the operon CEOP4020 on chromosome IV and cotranscribes with T07A9.7 and T07A9.9 (Fig. 2*A*). The *susi-2(ust49)* allele does not change the predicted ORF. We quantified mRNA levels of these three genes in *susi-2(ust49)* animals and found that the mRNA level of *susi-2* decreased to ∼20% of that of control animals (Fig. 2*A*), suggesting that the -1 guanosine-to-adenine mutation may affect *susi-2* pre-mRNA splicing or destabilize *susi-2* mRNA. We generated a CEOP4020 operon promoter-driven

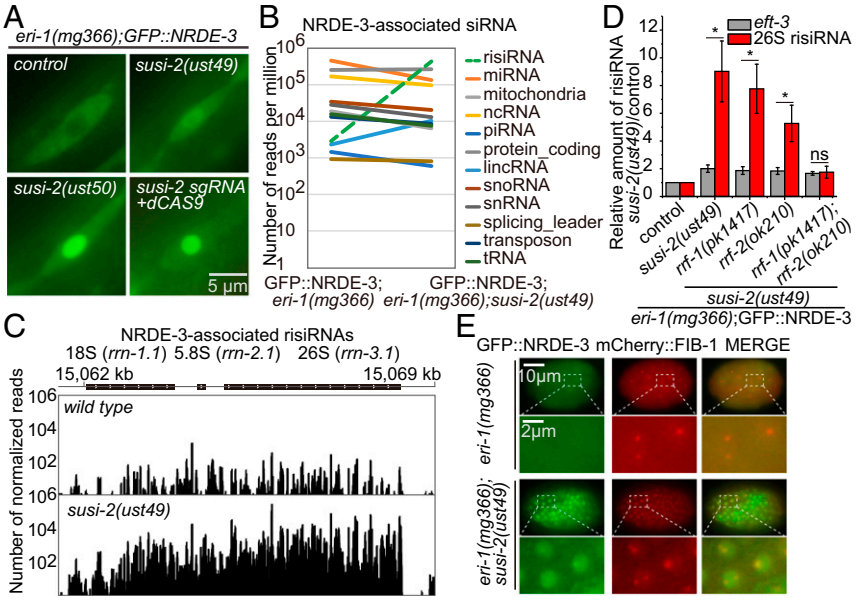

Fig. 1. risiRNAs accumulate in the *susi-2* mutants. (*A*) Images of representative seam cells of indicated animals. Animals were grown at 20 °C. (*B*) Deep sequencing of NRDE-3–associated siRNAs. The green dashed line indicates risiRNAs. Worms were cultured at 15 °C. (*C*) Distribution of NRDE-3–associated risiRNA reads across the rDNA locus. (*D*) qRT-PCR analysis of 26S risiRNAs in indicated animals at the L3 stage. Levels were normalized to *ama-1*. Mean ± SD ($n = 3$). Animals were grown at 20 °C. ns, Not significant. *$P <$ 0.05 (two-tailed Student's t test). (*E*) Images of *C. elegans* embryos of the indicated genotypes. Worms were cultured at 15 °C for two generations.

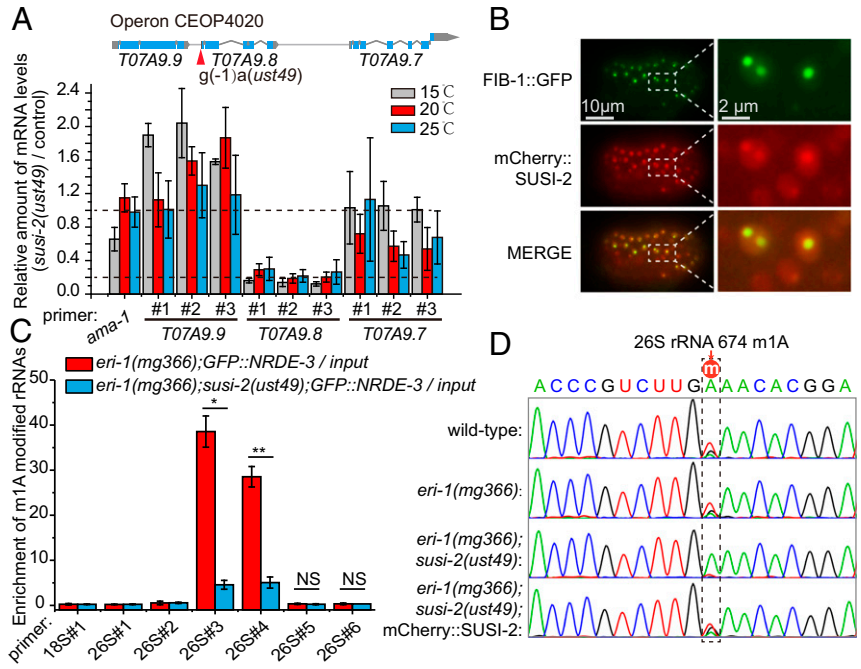

Fig. 2. SUSI-2 is required for the *N*1-methyladenosine modification of the 26S-A674 site. (*A*, *Lower*) qRT-PCR analysis of mRNA in *eri-1(mg366);susi-2(ust49);GFP::NRDE-3* animals at the L3 stage. Levels were normalized to *eft-3*. (*A*, *Upper*) The genomic structure of the operon CEOP4020. The location of the *susi-2(ust49)* allele is indicated. (*B*) Images of *C. elegans* embryos expressing FIB-1::GFP and mCherry::SUSI-2. (*C*) Quantification of m1A methylation levels in control and *susi-2(ust49)* animals at the L3 stage. The real-time PCR primer pairs are shown in Fig. 3*C* and *SI Appendix*, Fig. S2*C*. Mean ± SD ($n = 3$ animals). Two-tailed Student's *t* test in *A* and *C*. NS, Not significant. $^{*}P < 0.05$; $^{**}P < 0.01$. (*D*) Chromatogram of Sanger sequencing of the PCR-amplified cDNA sequence of 26S rRNA of indicated animals.

GFP::SUSI-2 transgene and found that SUSI-2 was expressed in almost all cells (*SI Appendix*, Fig. S2*A*). The mCherry::SUSI-2 colocalized with the nucleoli marker FIB-1::GFP, suggesting that SUSI-2 may function in the nucleolus (Fig. 2*B*).

SUSI-2 encodes an evolutionarily conserved protein exhibiting extensive homology to yeast and human RRP8 (*SI Appendix*, Fig. S2*B*). RRP8 is an *S*-adenosylmethionine–dependent methyltransferase responsible for m1A modification at the A645 site of yeast 25S rRNA (22). In *S. cerevisiae*, 25S rRNA contains two m1A modification sites, A645 and A2142 (23). In human cells, the 28S rRNAs harbor only one m1A modification at the A1322 site (23). In *C. elegans*, the predicted m1A methylation sites of 26S rRNAs are A674 and A2246 based on sequence homology to yeast 25S rRNA (*SI Appendix*, Fig. S2*C*). We designed a methylated RNA immunoprecipitation assay to quantify m1A methylation levels of rRNA. Total RNAs were isolated, chemically fragmented, immunoprecipitated with an anti-m1A antibody, and subjected to qRT-PCR (*SI Appendix*, Fig. S2*D*). m1A methylation at the A674 site of 26S rRNAs was enriched in wild-type animals but not in *susi-2(ust49)* animals (Fig. 2*C*). The mCherry::SUSI-2 transgene rescued A674-m1A methylation in the *susi-2(ust49)* mutant (*SI Appendix*, Fig. S2*E*). Interestingly, we failed to detect m1A methylation at the 26S-A2246 position.

*N*1-methylated adenosine disrupts the canonical Watson–Crick base pairing with thymine and causes both read-throughs to be accompanied by mismatch and reverse transcription stops (23). We used an m1A-induced misincorporation method to detect m1A sites in the 26S rRNA (24) and observed a pronounced mismatch rate at the A674 site in wild-type or *eri-1(mg366)* animals but not in *eri-1(mg366);susi-2(ust49)* mutants (Fig. 2*D*). The null allele *susi-2(ust50)* mutant displays a larval arrest phenotype, suggesting that the m1A modification at the A674 site of 26S rRNA may be crucial for animal growth and development.

Deficiency in m7G and m6(2)A Modifications Promotes risiRNA Generation. In addition to m1A, eukaryotic rRNAs contain a number of other modifications, including m7G, m5C, and m6(2)A, etc. We wondered whether defects in these rRNA modifications could similarly elicit the generation of risiRNAs. We selected nine predicted rRNA methyltransferases in *C. elegans* and acquired their mutants (*SI Appendix*, Fig. S3 *A* and *E* and Table S1). We used the subcellular localization of NRDE-3 as the reporter of risiRNA generation and examined whether the mutation of these methyltransferases can redistribute NRDE-3 from the cytoplasm to the nucleus. Two of these genes, *c27f2.4(ceBUD-23)* and *e02h1.1(ceDIMT1L)*, were identified in this screen. In the mutants, NRDE-3 redistributed from the cytoplasm to the nucleus (Fig. 3*A*).

C27F2.4(ceBUD-23) is a predicted guanine-*N*(7)-methyltransferase for the 18S rRNA-G1531 site (Fig. 3 *B* and *C*) (25). We confirmed the enrichment of risiRNAs in the *c27f2.4(tm5768)* mutant by using qRT-PCR (Fig. 3*D* and *SI Appendix*, Fig. S3*B*). Furthermore, both mature rRNAs and pre-rRNAs were significantly repressed in the *c27f2.4(tm5768)* mutant (Fig. 3*E*). Consistently, NRDE-3 associated with pre-rRNA in the *c27f2.4(tm5768)* mutant (*SI Appendix*, Fig. S3*C*). We designed an m7G RNA immunoprecipitation assay to quantify m7G methylation levels of rRNAs. Total RNAs were isolated, chemically fragmented, immunoprecipitated with an anti-m7G antibody, and subjected to qRT-PCR. We found that the m7G modification was enriched at the 18S-G1531 site in wild-type worms but not in the *c27f2.4(tm5768)* mutants (Fig. 3*F*). Additionally, the m7G modification levels were significantly decreased in the *c27f2.4* knockdown animals as well (*SI Appendix*, Fig. S3*D*).

E02H1.1(ceDIMT1L) is a predicted 18S rRNA m6(2)Am6(2)A-methyltransferase responsible for the methylation of the 18S-A1735 and -A1736 sites (*SI Appendix*, Fig. S3*F*) (26). We confirmed the enrichment of risiRNAs in *e02h1.1(ceDIMT1L)* knockdown animals by qRT-PCR (*SI Appendix*, Fig. S3*G*). Furthermore, both mature rRNAs and pre-rRNAs were significantly repressed in *e02h1.1* knockdown animals (*SI Appendix*, Fig. S3 *H* and *I*). Taken together, we concluded that the defects in rRNA modifications were able to elicit risiRNA production.

Genetic Screen-Identified risiRNAs Accumulated in the *susi-3(riok-1)* Mutant. One allele of *susi-3(ust51)* was isolated from the forward genetic screen. We identified *susi-3* as *riok-1(M01B12.5)* by SNP mapping followed by genome resequencing (*SI Appendix*, Fig. S4 *A* and *B*). A conserved amino acid, Ser149, in the kinase catalytic domain was mutated to leucine in RIOK-1*(ust51)*. RIOK-1 in *C. elegans* is homologous to yeast RIO1 and human RIOK1 that engage in 18S rRNA processing (*SI Appendix*, Fig. S4*B*) (27, 28). We acquired two additional alleles—*tm3775* from the National Bioresource Project and *ust52* by CRISPR-Cas9–mediated deletion (*SI Appendix*, Fig. S4 *A* and *B*). In all of the three alleles, NRDE-3 accumulated in the nucleus (Fig. 4*A*). A single-copy transgene of

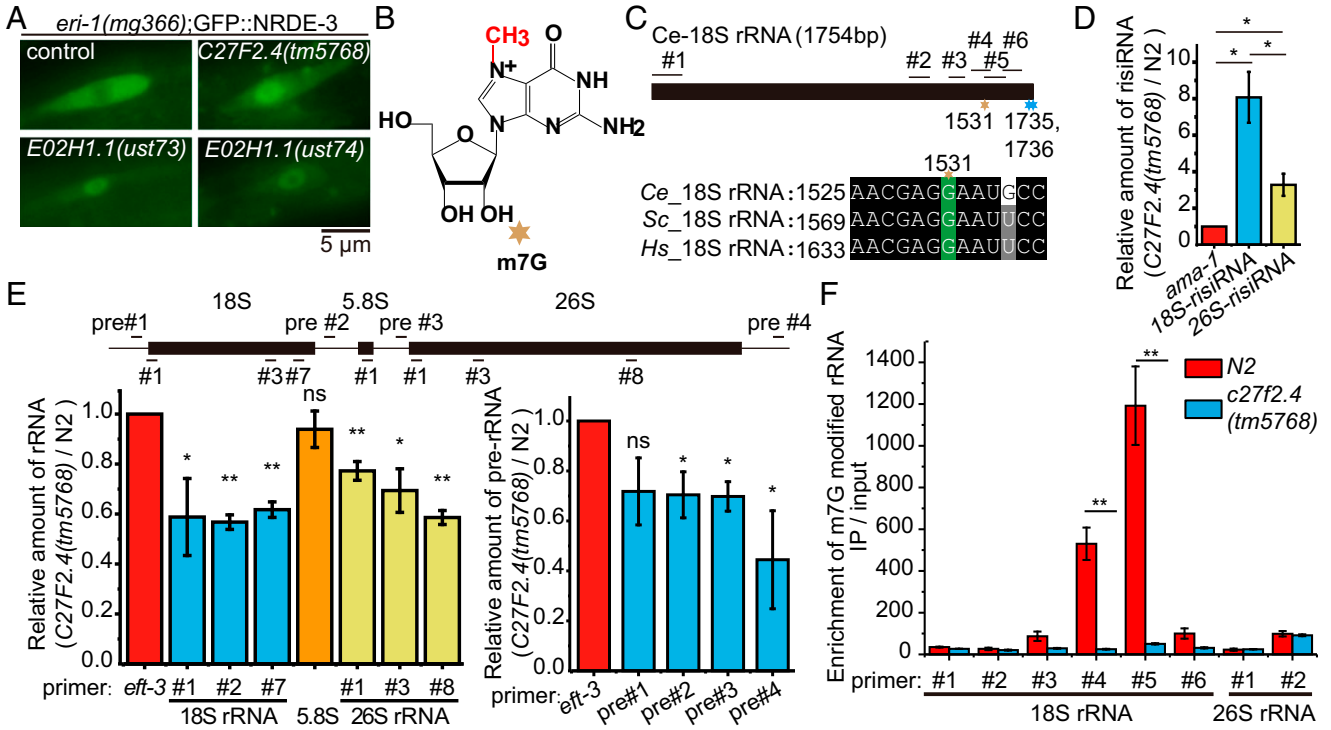

Fig. 3. Deficiency in rRNA modifications promotes risiRNA generation. (*A*) Images of seam cells of the indicated animals grown at 20 °C. (*B*) Chemical structure of 7-methylguanosine. (*C*) Schematic of the conserved m7G and m6(2)A sites in the 18S rRNA in *C. elegans*. The locations of primer pairs are indicated. Brown asterisks indicate m7G sites, and the blue asterisk indicates m6(2)A sites. Ce, *C. elegans*; Hs, *Homo sapiens*; Sc, *S. cerevisiae*. (*D*) Relative abundance of rRNAs and pre-rRNAs quantified by real-time PCR. Levels were normalized to *eft-3*. The location of primer pairs was indicated. (*E*) qRT-PCR analysis of 18S and 26S risiRNAs of L3-stage worms. Levels were normalized to *ama-1* mRNA. (*F*) Quantification of m7G methylation levels of L3-stage worms presented as the enrichment relative to input RNA. Mean ± SD ($n = 3$). Two-tailed Student's *t* test in *D*–*F*. ns, not significant. $^*P < 0.05$; $^{**}P < 0.01$.

mCherry::RIOK-1 rescued the cytoplasmic localization of NRDE-3 in *eri-1(mg366);susi-3(ust51)* animals (*SI Appendix*, Fig. S4*C*). We concluded that *susi-3* is *riok-1*, and therefore, we used *riok-1* in the following analyses.

We deep sequenced small RNAs either after NRDE-3 immunoprecipitation or from total RNA extraction in the *riok-1(ust51)* mutant. risiRNAs were enriched compared with the control strains (Fig. 4 *B* and *C* and *SI Appendix*, Fig. S4*D*). Additionally, in the *riok-1* mutant, NRDE-3 colocalized with mCherry::FIB-1 in nucleoli and associated with pre-rRNA (*SI Appendix*, Fig. S4 *E* and *F*). In addition, feeding *eri-1(mg366)* worms with exogenous dsRNA targeting *riok-1* down-regulated *riok-1* mRNA levels (*SI Appendix*, Fig. S4*G*) and increased risiRNA sequences complementary to 18S and 26S rRNAs (Fig. 5*B* and *SI Appendix*, Fig. S4*H*). We tested whether risiRNAs were able to silence rRNAs or pre-rRNAs in *riok-1* knockdown animals and found that both mature rRNAs and pre-rRNAs were decreased after treatment with RNAi targeting *riok-1* (Fig. 4 *D* and *E*).

Both yeast RIO1 and human RIOK1 engage in 18S rRNA processing in the cytoplasm (27, 28). Similarly, RIOK-1 in *C. elegans* localized to the cytoplasm in larva and embryos in both soma and germline cells (*SI Appendix*, Fig. S5*A*). Interestingly, RIOK-1 could translocate from the cytoplasm to nucleus during cell division in early embryos (*SI Appendix*, Fig. S5*B*), which has also been observed for yeast RIO1 (29). We tested whether the mutation of other *susi* genes affects the subcellular localization of RIOK-1 but failed to find any change in the *susi-2(ust49)* and *c27f2.4(tm5768)* mutants (*SI Appendix*, Fig. S5 *C* and *D*).

rRNA Processing Deficiencies Promote the Generation of risiRNAs. To further test whether erroneously processed rRNAs can promote risiRNA generation, we used an risiRNA sensor (*SI Appendix*, Fig. S6*A*) and performed a candidate screen to search for rRNA processing factors that are able to suppress risiRNA production. We selected 59 predicted rRNA processing factors and investigated whether knocking down these genes by RNAi can silence the risiRNA sensor because of the increase of risiRNAs (*SI Appendix*, Table S2). RNAi targeting for 8 of 59 genes, including *susi-2* and *riok-1*, was able to silence the risiRNA sensor but not the control sensor (*SI Appendix*, Fig. S6*B* and Table S3). We deleted three of the genes, *crn-3*, *t22h9.1*, and *zk686.2*, by CRISPR-Cas9 technology (*SI Appendix*, Fig. S6*C*) and acquired the *rha-2(ok2639)* mutant from CGC. In these mutants, NRDE-3 redistributed from the cytoplasm to the nucleus (Fig. 5*A*). We further confirmed the enrichment of risiRNAs in *crn-3*, *t22h9.1*, *zk686.2*, and *rha-2* knockdown animals by qRT-PCR (Fig. 5*B*). These results suggested that deficiencies in rRNA processing were able to promote risiRNA generation.

The *susi* mutants grew slower and were usually arrested at the larval stage, which is consistent with the essential roles of rRNAs for the development of multicellular organisms (*SI Appendix*, Fig. S7*A* and Table S4). To specifically examine the physiological roles of risiRNAs, we investigated the developmental progress of *susi* mutants. Gravid adult animals were allowed to lay eggs for 1 h, and the growth of progeny was monitored at 20 °C. Compared with control animals, the *susi* mutants exhibited a slower growth rate, which could be partially rescued in the *rrf-1;rrf-2* double-mutant background (Fig. 5*C* and *SI Appendix*, Fig. S7*B*). Noticeably, the *susi-2(ust49)*, *c27f2.4(tm5768)*, and *riok-1(ust49)* mutants did not exhibit pronounced brood size defects at 20 °C but did show some synergistic defects in RdRP or *nrde-3* mutated background (*SI Appendix*, Fig. S7 *C* and *D*). We conclude that risiRNAs may play important roles in animal development.

We further examined the generation of risiRNAs in seam cells. *C. elegans* has 16 seam cells in larval 4 (L4) stage. GFP::NRDE-3 accumulated in the nucleus in most of the seam cells in *susi* mutants (*SI Appendix*, Fig. S7*E*). However, we observed that GFP::NRDE-3 accumulated in the cytoplasm in a number of seam cells in the mutant animals. We speculated that the amplification

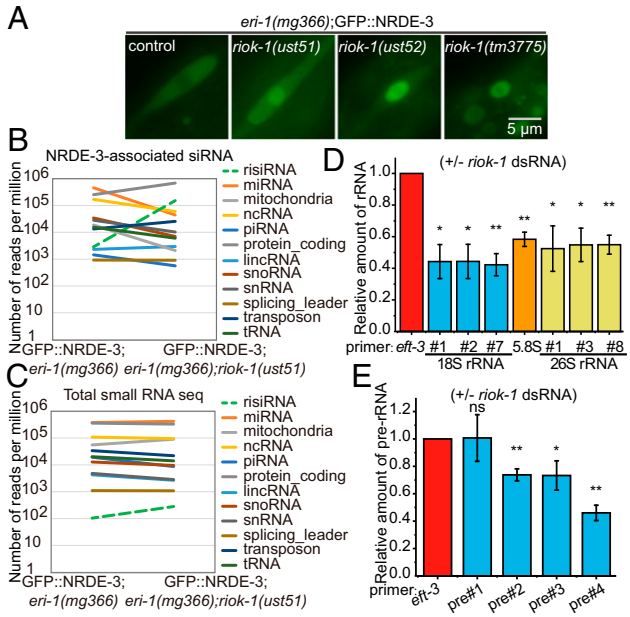

Fig. 4. risiRNA accumulates in the *susi-3(riok-1)* mutant. (*A*) Images of seam cells of the indicated animals grown at 20 °C. (*B*) Deep sequencing of NRDE-3–associated siRNAs in control and *riok-1(ust51)* animals at the L3-stage grown at 15 °C. The green dashed line indicates risiRNAs. (*C*) Deep sequencing of total small RNAs in control and *riok-1(ust51)* animals at the L3-stage grown at 15 °C. (*D* and *E*) Relative abundance of (*D*) rRNA and (*E*) pre-rRNA quantified by real-time PCR in control and *riok-1(RNAi)* animals under *eri-1(mg366)* background at the L3 stage. Levels were normalized to *eft-3*. Mean ± SD ($n = 3$). Two-tailed Student's *t* test. ns, not significant. $*P < 0.05$; $**P < 0.01$.

efficacy of risiRNAs by RdRPs could be different among individual cells, possibly because of stochastic reasons.

Discussion

To avoid accumulation of unnecessary and potentially harmful transcripts, cells have developed a number of RNA surveillance systems by engaging exosomes and other exoribonucleases (4, 8–10, 13, 14, 30). Here, we have described a mechanism to prohibit the accumulation of erroneous rRNAs. When rRNA modification or splicing processes are impaired, the erroneous rRNAs may accumulate and promote the generation of risiRNAs, which can, in turn, silence pre-rRNA expression via the nuclear RNAi pathway. The risiRNA/RNAi-directed feedback loop, therefore, may compensate for the dysfunction of exoribonuclease-engaged degradation of erroneous rRNAs (*SI Appendix*, Fig. S8).

Deficiencies in rRNA Modifications and Processing Promote the Generation of risiRNAs. rRNAs are modified by a number of enzymes at different stages throughout the biogenesis of ribosomes. These modifications can stabilize the secondary and tertiary structures of the rRNA scaffold and ensure the efficiency and accuracy of polypeptide synthesis (6, 7, 31). While the mechanisms regulating rRNA modifications are largely unknown, changes in the rRNA modifications have been observed in response to environmental stimuli, during development, and in certain diseases.

Here, we showed that the defects in rRNA modification enzymes and a deficiency in rRNA modifications could trigger the generation of risiRNAs, which utilize the RNAi silencing pathway to inhibit the accumulation of erroneous rRNAs. We confirmed that SUSI-2 is a methyltransferase responsible for the *N*1-methyladenosine modification of the 26S rRNA and that C27F2.4(ceBUD23) is involved in modifying the 7-methylguanine of the 18S rRNA by an RNA methylation—immunoprecipitation assay. The identification of these enzymes will facilitate additional investigation of the biological roles and regulations of rRNA modifications in *C. elegans*. In addition, identification of their endogenous substrates other than rRNAs will expand our knowledge of RNA modifications and RNAomics.

Splicing Errors in rRNAs Elicit the Generation of risiRNAs. In eukaryotic cells, rRNAs are transcribed by RNA polymerase I into a single 47S polycistronic precursor in the nucleolus. Pre-rRNAs are then modified, processed, folded, and matured into 18S, 5.8S, and 28S rRNA (4). These splicing steps are precisely orchestrated by distinct enzymes and a number of intermediate complexes (32). Here, we identified SUSI-3(ceRIOK-1) and other pre-rRNA processing factors in *C. elegans*. When mistakes occur in rRNA splicing, incorrectly processed rRNAs may accumulate and by mechanisms unknown, recruit RdRPs to initiate the production of risiRNAs.

risiRNAs Silence Pre-rRNA via the Nuclear RNAi Pathway. risiRNAs suppress rRNA at least in part through the nuclear RNAi pathway. Small RNAs targeting protein coding genes have been shown to recruit the NRDE complex to the targeted nascent transcripts, induce H3K9me3 and H3K27me3 modifications, pause RNA polymerase II, and induce a premature termination of transcription. When animals are fed with exogenous dsRNA targeting rRNAs and in the *susi-1(ceDisL2)* mutants, risiRNAs accumulate and elicit an association of the nuclear Argonaute NRDE-3 with pre-rRNA transcripts (18). It will be very interesting to test whether risiRNAs modulate rRNA transcription via similar

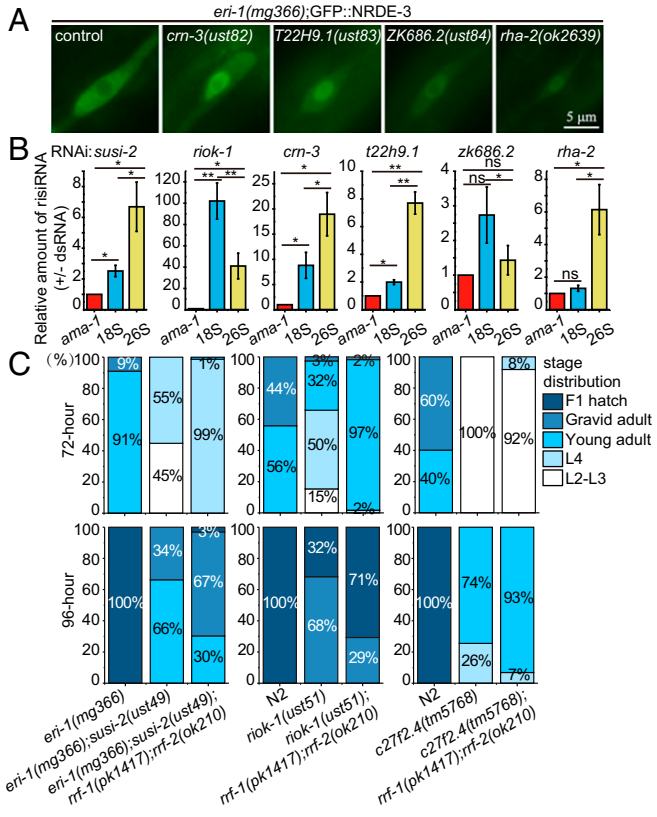

Fig. 5. The defects in rRNA processing promote risiRNA generation. (*A*) Images of seam cells of indicated animals grown at 20 °C at the L3 stage. (*B*) qRT-PCR analysis of 18S and 26S risiRNAs after knocking down indicated genes for two generations in *eri-1(mg366)* animals. Total RNA samples were collected at the L3 stage. Expression levels were normalized to *ama-1*. Mean ± SD ($n = 3$). Two-tailed Student's *t* test. ns, not significant. $*P < 0.05$; $**P < 0.01$. (*C*) Developmental progress of indicated animals. The developmental stage of animals was monitored every 24 h at 20 °C ($n > 50$).

mechanisms. Since small RNA-directed H3K9me3 is dispensable for nuclear RNAi-mediated gene silencing when targeting protein coding genes, identifying which types of histone modifications are related to rDNA silencing will be very important to understand the mechanism and regulation of risiRNAs (33, 34).

The Physiological Roles of risiRNA. Endogenous metabolic stressors and environmental stimuli can elicit RNA processing disorders, lead to the accumulation of erroneous RNAs, and result in developmental and metabolic disorders (30). Ribosomopathies describe a number of disorders in which genetic abnormalities can cause impaired ribosome biogenesis and function and result in specific clinical phenotypes (35, 36). The detailed mechanisms between rRNA processing disorders and ribosomopathies are largely unclear. Previously, we showed that lower temperature and UV irradiation could impair 3′-end maturation of the 26S rRNA, trigger risiRNA expression, and down-regulate pre-rRNA (16). It is possible that environmental stimuli can trigger certain signaling pathways to elicit risiRNA production. Alternatively, the defects in rRNA degradation can result in risiRNA generation. In this work, we showed that risiRNAs accumulate in response to rRNA processing and modification errors. Therefore, we speculate that the risiRNA/RNAi-directed feedback loop may compensate for the dysfunction of exoribonuclease-engaged degradation of erroneous rRNAs and sustain animal development. It is unclear how different types of erroneous rRNAs are detected. Additional elucidation of the mechanisms will assist our understanding of the quality control of rRNAs and ribosomes and provide therapeutic strategies for human diseases.

Materials and Methods

Strains. Bristol strain N2 was used as the standard wild-type strain. The Hawaiian strain CB4856 was used for snp-SNP mapping. All strains were incubated at 20 °C unless otherwise specified. The strains used in this study are listed in *SI Appendix*, Table S5. The construction of mutants and transgenes is described in detail in *SI Appendix*.

Genetic Screen and RNAi. Genetic screen experiments were conducted as previously described (16). RNAi experiments were conducted as previously described (37).

Quantification of the Subcellular Location of NRDE-3. The subcellular localization of NRDE-3 was quantified as described previously (16). For the 15 °C and 25 °C treatments, worms were cultured at 15 °C or 25 °C from embryonic to L3 stage. For analyzing the nucleolar foci of NRDE-3 in embryos in *susi-2* and *susi-3* mutants, worms were cultured in 15 °C for at least two generations.

Quantification of RNA Methylation. Methylated RNAs were immunoprecipitated and quantified as described previously (23, 38). Briefly, total RNA was isolated from indicated animals and fragmented into ∼150-nt pieces. RNA was purified, immunoprecipitated with anti-m1A antibody, and eluted with 6.7 mM *N*1-methyladenosine. The RNA was purified again and quantified by qRT-PCR. For m7G detection, the m7G antibody was used, and the antibody-bound RNA was purified via the phenol/chloroform extracting method. The experimental procedures are described in detail in *SI Appendix*.

Deep Sequencing of Small RNAs and Bioinformatics. Total RNA was isolated from L3-stage worms and subjected to small RNA deep sequencing using an Illumina platform (Novogene Bioinformatics Technology Co., Ltd.). The experimental procedure and data analysis are described in detail in *SI Appendix*.

Statistics. Bar graphs with error bars are presented with means and SDs. All of the experiments were conducted with independent *C. elegans* animals for an indicated *N* times. Statistical analysis was performed with the two-tailed Student's *t* test.

ACKNOWLEDGMENTS. We thank the members of the laboratory of S.G. for their comments. We also thank the International *Caenorhabditis elegans* Gene Knockout Consortium and the National Bioresource Project for providing the strains. Some strains were provided by the Caenorhabditis Genetics Center (CGC), which is funded by NIH Office of Research Infrastructure Programs Grant P40 OD010440. This work was supported by Chinese Ministry of Science and Technology Grant 2017YFA0102903; National Natural Science Foundation of China Grants 81501329, 31671346, and 91640110; Anhui Natural Science Foundation Grants 1608085MC50 and 1808085QC82; and Major/Innovative Program of Development Foundation of Hefei Center for Physical Science and Technology Grant 2017FXZY005.

1. Lafontaine DL (2015) Noncoding RNAs in eukaryotic ribosome biogenesis and function. *Nat Struct Mol Biol* 22:11–19.
2. Xue S, Barna M (2012) Specialized ribosomes: A new frontier in gene regulation and organismal biology. *Nat Rev Mol Cell Biol* 13:355–369.
3. Greber BJ (2016) Mechanistic insight into eukaryotic 60S ribosomal subunit biogenesis by cryo-electron microscopy. *RNA* 22:1643–1662.
4. Henras AK, Plisson-Chastang C, O'Donohue MF, Chakraborty A, Gleizes PE (2015) An overview of pre-ribosomal RNA processing in eukaryotes. *Wiley Interdiscip Rev RNA* 6:225–242.
5. Woolford JL, Jr, Baserga SJ (2013) Ribosome biogenesis in the yeast Saccharomyces cerevisiae. *Genetics* 195:643–681.
6. Sloan KE, et al. (2017) Tuning the ribosome: The influence of rRNA modification on eukaryotic ribosome biogenesis and function. *RNA Biol* 14:1138–1152.
7. Sharma S, Lafontaine DLJ (2015) 'View from a bridge': A new perspective on eukaryotic rRNA base modification. *Trends Biochem Sci* 40:560–575.
8. Peña C, Hurt E, Panse VG (2017) Eukaryotic ribosome assembly, transport and quality control. *Nat Struct Mol Biol* 24:689–699.
9. Lafontaine DL (2010) A 'garbage can' for ribosomes: How eukaryotes degrade their ribosomes. *Trends Biochem Sci* 35:267–277.
10. Schmidt K, Butler JS (2013) Nuclear RNA surveillance: Role of TRAMP in controlling exosome specificity. *Wiley Interdiscip Rev RNA* 4:217–231.
11. Fox MJ, Mosley AL (2016) Rrp6: Integrated roles in nuclear RNA metabolism and transcription termination. *Wiley Interdiscip Rev RNA* 7:91–104.
12. Thoms M, et al. (2015) The exosome is recruited to RNA substrates through specific adaptor proteins. *Cell* 162:1029–1038.
13. Vanacova S, Stefl R (2007) The exosome and RNA quality control in the nucleus. *EMBO Rep* 8:651–657.
14. Houseley J, LaCava J, Tollervey D (2006) RNA-quality control by the exosome. *Nat Rev Mol Cell Biol* 7:529–539.
15. Lubas M, et al. (2013) Exonuclease hDIS3L2 specifies an exosome-independent 3′-5′ degradation pathway of human cytoplasmic mRNA. *EMBO J* 32:1855–1868.
16. Zhou X, Chen X, Wang Y, Feng X, Guang S (2017) A new layer of rRNA regulation by small interference RNAs and the nuclear RNAi pathway. *RNA Biol* 14:1492–1498.
17. Guang S, et al. (2008) An Argonaute transports siRNAs from the cytoplasm to the nucleus. *Science* 321:537–541.
18. Zhou X, et al. (2017) RdRP-synthesized antisense ribosomal siRNAs silence pre-rRNA via the nuclear RNAi pathway. *Nat Struct Mol Biol* 24:258–269.
19. Long L, et al. (2015) Regulation of transcriptionally active genes via the catalytically inactive Cas9 in C. elegans and D. rerio. *Cell Res* 25:638–641.
20. Gu W, et al. (2009) Distinct Argonaute-mediated 22G-RNA pathways direct genome surveillance in the C. elegans germline. *Mol Cell* 36:231–244.
21. Lee LW, Lee CC, Huang CR, Lo SJ (2012) The nucleolus of Caenorhabditis elegans. *J Biomed Biotechnol* 2012:601274.
22. Peifer C, et al. (2013) Yeast Rrp8p, a novel methyltransferase responsible for m1A 645 base modification of 25S rRNA. *Nucleic Acids Res* 41:1151–1163.
23. Dominissini D, et al. (2016) The dynamic N(1)-methyladenosine methylome in eukaryotic messenger RNA. *Nature* 530:441–446.
24. Li X, et al. (2017) Base-resolution mapping reveals distinct m1A methylome in nuclear- and mitochondrial-encoded transcripts. *Mol Cell* 68:993–1005.e9.
25. White J, et al. (2008) Bud23 methylates G1575 of 18S rRNA and is required for efficient nuclear export of pre-40S subunits. *Mol Cell Biol* 28:3151–3161.
26. Zorbas C, et al. (2015) The human 18S rRNA base methyltransferases DIMT1L and WBSCR22-TRMT112 but not rRNA modification are required for ribosome biogenesis. *Mol Biol Cell* 26:2080–2095.
27. Turowski TW, et al. (2014) Rio1 mediates ATP-dependent final maturation of 40S ribosomal subunits. *Nucleic Acids Res* 42:12189–12199.
28. Widmann B, et al. (2012) The kinase activity of human Rio1 is required for final steps of cytoplasmic maturation of 40S subunits. *Mol Biol Cell* 23:22–35.
29. Iacovella MG, et al. (2015) Rio1 promotes rDNA stability and downregulates RNA polymerase I to ensure rDNA segregation. *Nat Commun* 6:6643.
30. Karbstein K (2013) Quality control mechanisms during ribosome maturation. *Trends Cell Biol* 23:242–250.
31. Natchiar SK, Myasnikov AG, Kratzat H, Hazemann I, Klaholz BP (2017) Visualization of chemical modifications in the human 80S ribosome structure. *Nature* 551:472–477.
32. Wan R, Yan C, Bai R, Lei J, Shi Y (2017) Structure of an intron lariat spliceosome from Saccharomyces cerevisiae. *Cell* 171:120–132.e12.
33. Mao H, et al. (2015) The Nrde pathway mediates small-RNA-directed histone H3 lysine 27 trimethylation in Caenorhabditis elegans. *Curr Biol* 25:2398–2403.
34. Kalinava N, Ni JZ, Peterman K, Chen E, Gu SG (2017) Decoupling the downstream effects of germline nuclear RNAi reveals that H3K9me3 is dispensable for heritable RNAi and the maintenance of endogenous siRNA-mediated transcriptional silencing in *Caenorhabditis elegans*. *Epigenetics Chromatin* 10:6.
35. Narla A, Ebert BL (2010) Ribosomopathies: Human disorders of ribosome dysfunction. *Blood* 115:3196–3205.
36. Mills EW, Green R (2017) Ribosomopathies: There's strength in numbers. *Science* 358: eaan2755.
37. Timmons L, Court DL, Fire A (2001) Ingestion of bacterially expressed dsRNAs can produce specific and potent genetic interference in *Caenorhabditis elegans*. *Gene* 263:103–112.
38. Li X, et al. (2016) Transcriptome-wide mapping reveals reversible and dynamic N(1)-methyladenosine methylome. *Nat Chem Biol* 12:311–316.